Thievessen et al., http://www.jcb.org/cgi/content/full/jcb.201303129/DC1

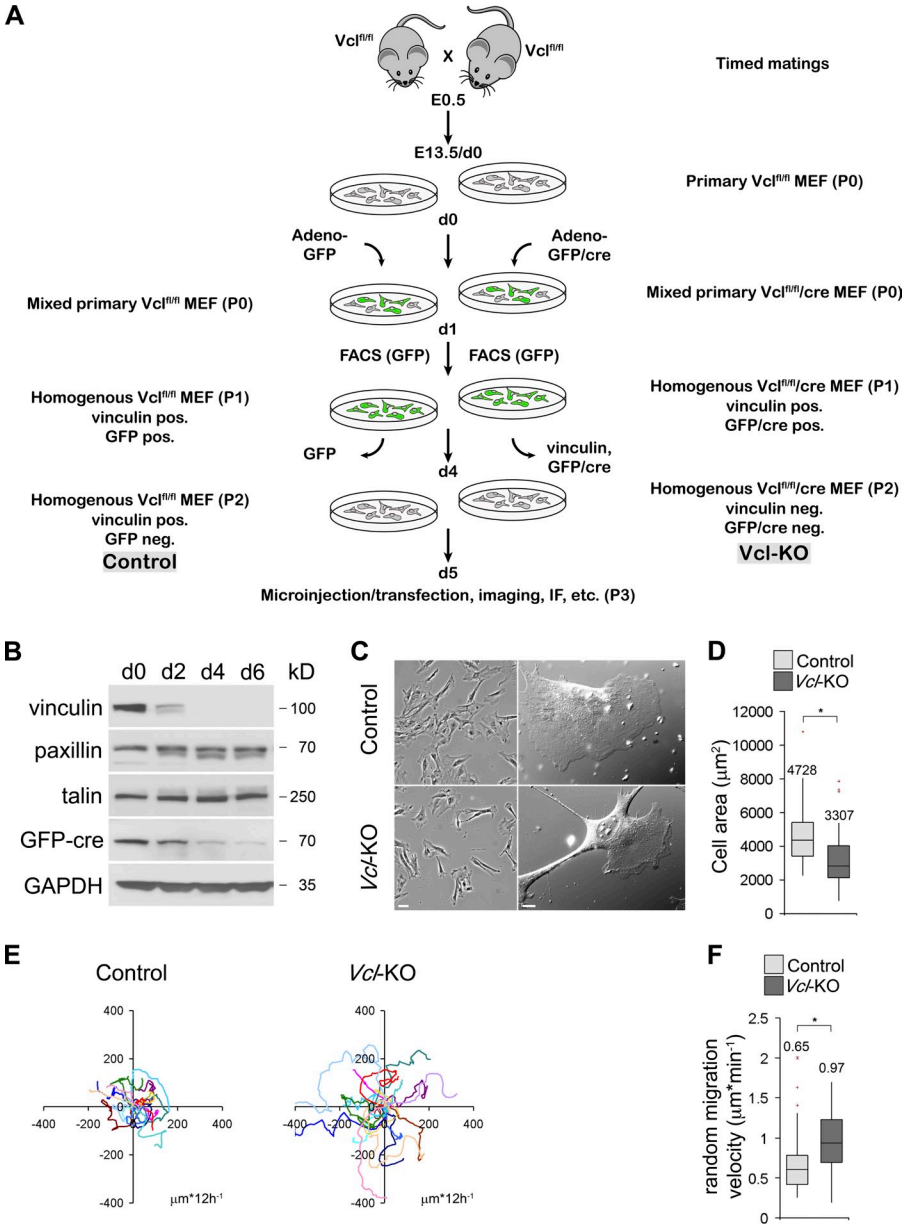

Figure S1. **Generation and basic characterization of primary vinculin-deficient MEF from Vcl$^{fl/fl}$ mice.** (A) Primary MEF were isolated from E13.5 Vcl$^{fl/fl}$ mouse embryos, obtained from timed matings of Vcl$^{fl/fl}$ mice, and infected with a GFP/cre-expressing adenovirus to delete essential sequences of *Vcl* in vitro (Zemljic-Harpf et al., 2007). Control cells from the same primary culture were generated by infection with an adenovirus expressing GFP. To generate homogenous populations of vinculin-depleted and control MEF, primary cultures were GFP FAC sorted and subsequently cultured until the complete loss of remaining vinculin protein and GFP/cre or GFP, respectively. Cells were used for experiments on days 5–7, passage 3. (B) Western blot of vinculin, paxillin, talin, GFP-cre, and GAPDH (loading control) in lysates of Vcl$^{fl/fl}$ MEF infected with GFP-cre recombinase-expressing adenovirus. (C) Phase-contrast (left) and DIC (right) micrographs of live control and *Vcl*-KO MEF. Bars: (left) 50 µm; (right) 10 µm. (D) Box and whisker plot of cell area, 24 h after plating on 10 mg/ml FN-coated coverslips; $n = 23$ (control) and $n = 35$ (*Vcl*-KO) MEF; means indicated; *, $P < 0.01$, Student's *t* test. (E) Representative tracks of 15 control and 15 *Vcl*-KO MEF, randomly migrating on 10 mg/ml FN-coated coverslips, monitored for 12 h at 10-min frame rate. (F) Box and whisker plot of random cell migration velocity on FN; $n = 93$ (control) and $n = 111$ (*Vcl*-KO) MEF; means indicated; *, $P < 0.001$, Student's *t* test.

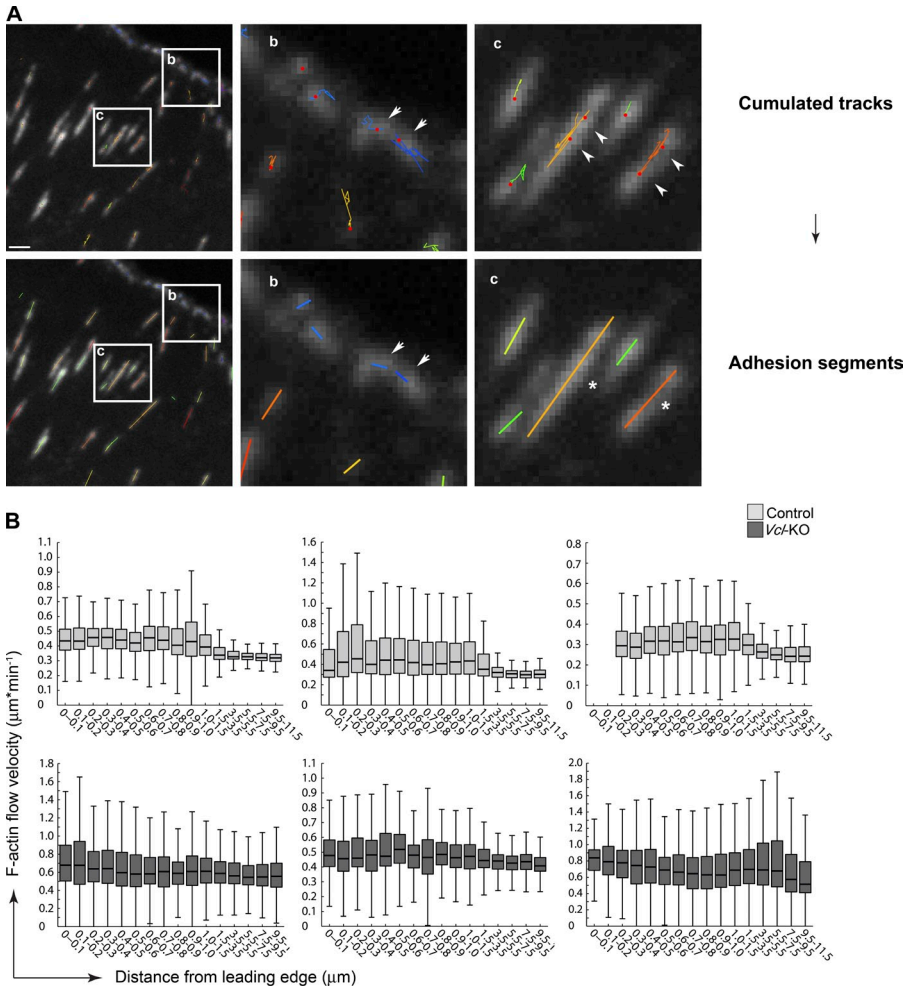

Figure S2. **Detection and tracking of local intensity maxima of nascent and maturing FA on SDC time-lapse image sequences of EGFP-paxillin expressing MEF.** (A) Tracks (top) were grouped based on their relative proximity and alignment (see Materials and methods for details) to reconstruct FA over time (bottom). Overview of cumulated tracks and corresponding FA segments at the protruding front of a control MEF (left). (A, b) Zoom of regions showing tracks and segments of nascent FA (blue) at the outermost leading edge. Note separate FA segments generated from nearby tracks of individual nascent FA (arrows). (A, c) Zoom of regions showing tracks and segments of maturing FA in the lamellum. Note grouping of nearby tracks from the same FA (arrowheads) into one FA segment (asterisks). Bar, 1 µm. (B) Vinculin is required to attenuate F-actin flow in lamellipodial FA. Box and whisker plots of retrograde F-actin flow velocity within automatically segmented FA as a function of the distance to the leading edge. The center of each box shows the median. Whiskers extend from the 25th and 75th percentile to the most extreme data points not considered outliers by the algorithm. Shown are the distributions of three representative control and *Vcl*-KO MEF during protrusion phases. Note the sudden drop of F-actin flow velocities in FA of control MEF at distances of ~1.5 µm away from the leading edge, compared with a slow, continuous reduction of F-actin flow velocities in FA of *Vcl*-KO MEF. The drop of F-actin flow velocities in control FA was accompanied by a homogenized flow distribution (strongly reduced extension of boxes and whiskers), indicating that the zone at the cell front consists of actin structures with a wide range of differential engagement at FA (Ponti et al., 2004). This zone is significantly broader in *Vcl*-KO MEF.

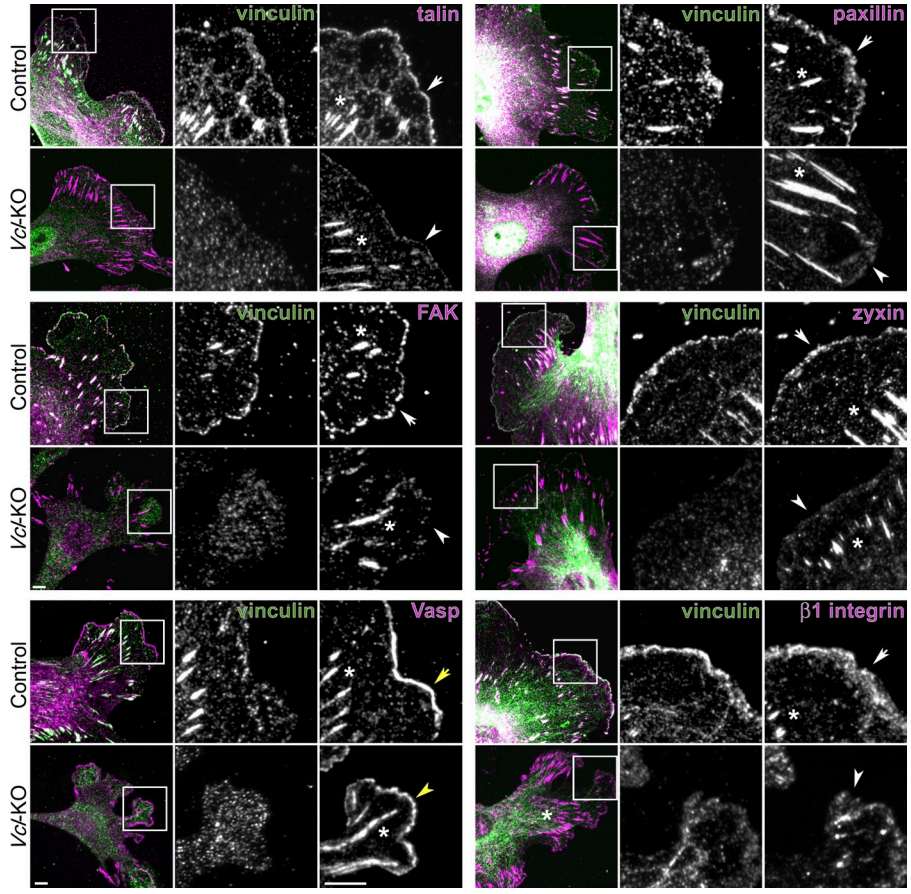

Figure S3. **Loss of vinculin affects small, peripheral FA and mature FA differently.** SDC micrographs of control and *Vcl*-KO MEF, immunofluorescence stained for vinculin and the indicated FA proteins. Note elongated, mature FA present in both control and *Vcl*-KO MEF (asterisks) and peripheral immature FA containing talin, paxilin, FAK, zyxin, and β1 integrin, abundant in control (white arrow) but not *Vcl*-KO (white arrowhead) MEF. Note VASP localization at the leading edge of cell protrusions in both control (yellow arrow) and *Vcl*-KO (yellow arrowhead) MEF. Bars, 10 µm.

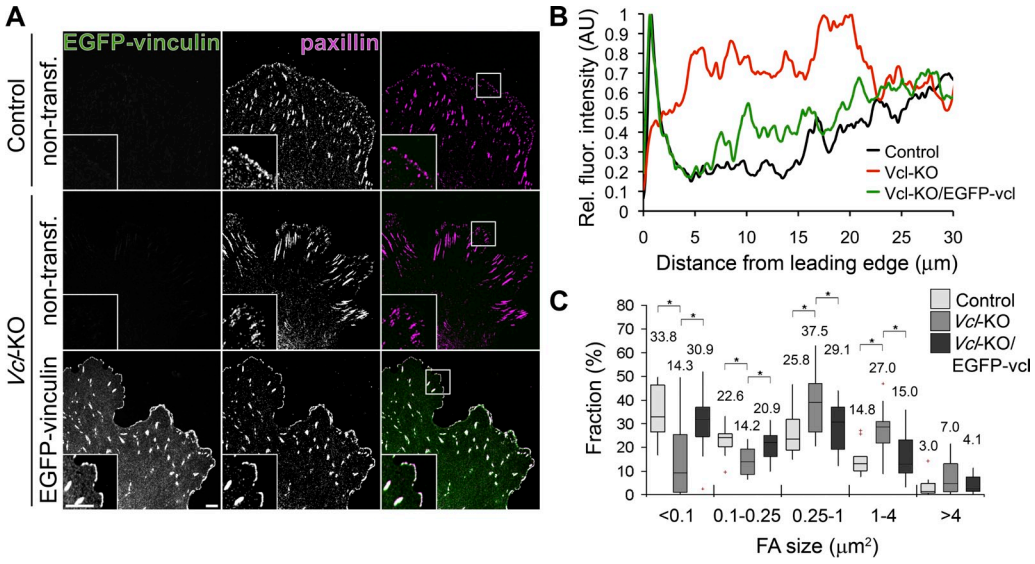

Figure S4. **Reexpression of full-length vinculin restores nascent FA and normal FA organization in *Vcl*-KO MEF.** (A) Paxillin immunofluorescence staining (purple) of control MEF and nontransfected as well as EGFP-vinculin (green)–transfected *Vcl*-KO MEF. EGFP-vinculin expression is shown in left panels. Bars, 5 µm. (B) Paxillin fluorescence intensity distribution along line scans perpendicular to the leading edge (mean of 10 cells for each condition). (C) Box and whisker plot of FA size distribution in $n = 10$ cells for each condition with FA marker paxillin; means indicated; *, $P < 0.05$, Mann-Whitney *U* test.

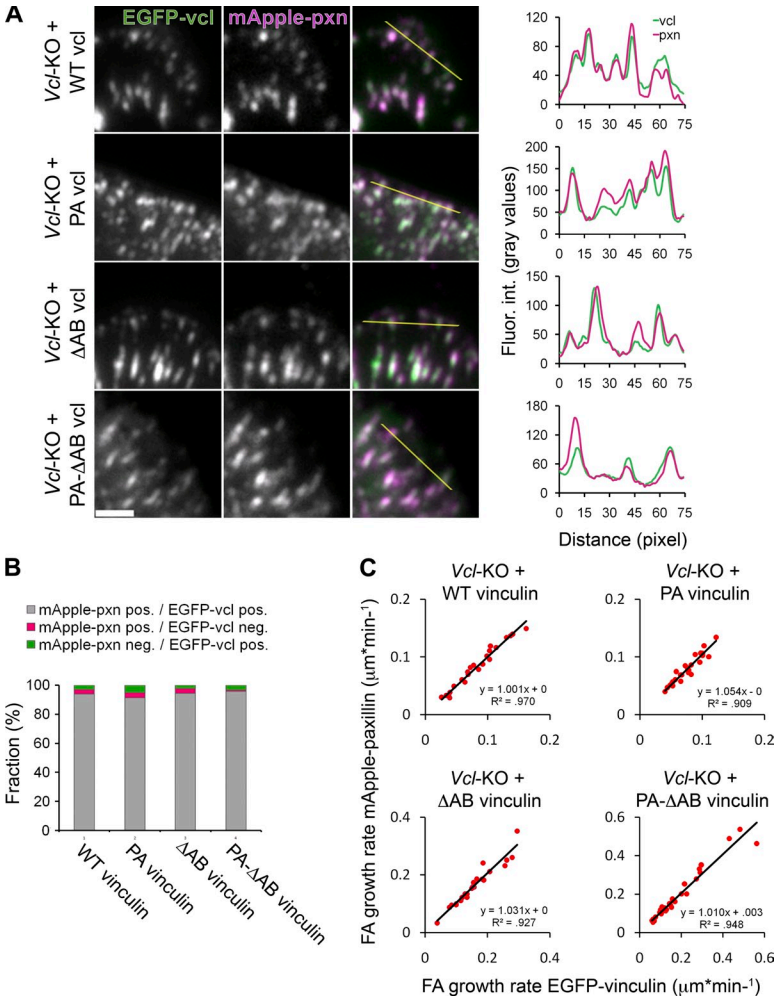

Figure S5. **Colocalization of EGFP-vinculin mutants with mApple-paxillin in nascent FA and comparable FA growth rates measured by FA labeling with mApple-paxillin and EGFP-vinculin mutants.** (A) TIRF micrographs of live *Vcl*-KO MEF expressing the indicated EGFP-vinculin cDNA and mApple-paxillin to label nascent FA (Choi et al., 2008). Line scans through areas of nascent FA showing colocalization of WT, PA, ΔAB, and PA-ΔAB vinculin with paxillin. Bar, 2 µm. (B) Bar diagram showing the fractions of nascent FA positive for mApple-paxillin and the indicated EGFP-vinculin variants (gray) or for either mApple-paxillin (purple) or the respective EGFP-vinculin variant (green) only. The constructs were cotransfected into *Vcl*-KO MEF and TIRF images were taken from live cells. 93.9 ± 3.0% (WT), 91.3 ± 3.4% (PA), 94.4 ± 3.2% (ΔAB), and 95.9 ± 0.8% (PA-ΔAB) of nascent FA counted were positive for mApple-paxillin and the respective EGFP-vinculin mutant; $n > 100$ nascent FA of three to five cells per condition. (C) Plots of growth rates of individual FA in *Vcl*-KO MEF expressing mApple-paxillin and the indicated EGFP-vinculin mutant cDNA, measured on the same kymograph in the paxillin and vinculin channel. Note linear regression of approximately one for the correlation between FA growth rates based on paxillin and vinculin labeling for each condition; n = 24 (WT), n = 26 (PA), n = 25 (ΔAB), and n = 31 (PA-ΔAB) FA from three to six cells per condition. SDC confocal time-lapses at 20-s frame rate.

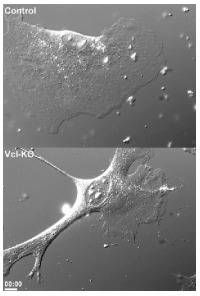

Video 1. **Morphology of live control and *Vcl*-KO MEF.** DIC time-lapse image sequences of control and *Vcl*-KO MEF. Images were taken every 5 s (elapsed time shown in min:s) on an inverted microscope system (TE300; Nikon) using a 60×/1.49 NA Apo TIRF objective lens. Bar, 10 µm.

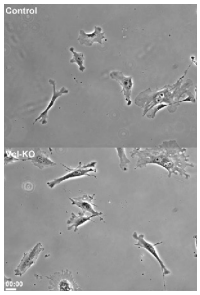

Video 2. **Random migration of control and *Vcl*-KO MEF.** Phase-contrast time-lapse image sequences of migrating control and *Vcl*-KO MEF. Images were taken every 10 min (elapsed time shown in h:min) on an inverted microscope system (TE300; Nikon) using a 10×/0.25 NA Plan objective lens. Bar, 50 µm.

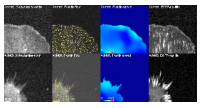

Video 3. **F-actin dynamics in control and *Vcl*-KO MEF.** SDC-FSM time-lapse image sequences of F-actin and FA dynamics in control and *Vcl*-KO MEF microinjected with X-rhodamine actin and EGFP-paxillin cDNA. (left to right) X-rhodamine actin FSM images, F-actin flow maps, F-actin speed maps, and EGFP-paxillin. Images were taken every 10 s (elapsed time shown in min:s) on an inverted microscope system (TE2000E2; Nikon) using a 100×/1.49 NA Apo TIRF objective lens. Bars: 2 µm; (flow scale) 2 µm*min^{-1}; (speed scale) nm*min^{-1}.

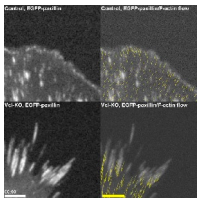

Video 4. **Overlay of F-actin flow and FA in control and *Vcl*-KO MEF.** SDC fluorescence time-lapse image sequences of FA (EGFP-paxillin; left), overlayed with F-actin flow maps (right) in control and *Vcl*-KO MEF. Images were taken every 10 s (elapsed time shown in min:s) on an inverted microscope system (TE2000E2; Nikon) using a 100×/1.49 NA Apo TIRF objective lens. Bars: 2 µm; (flow scale) 2 µm*min^{-1}.

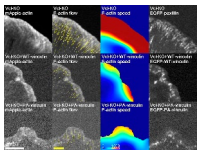

Video 5. **F-actin dynamics in *Vcl*-KO MEF expressing EGFP-WT or -PA vinculin.** SDC-FSM time-lapse image sequences of F-actin and FA dynamics in *Vcl*-KO MEF coexpressing mApple-actin and either EFGP-paxillin (nonrescued; top), EGFP-WT (middle), or EGFP-PA (bottom) vinculin cDNA. (left to right) mApple-actin FSM images, F-actin flow maps, F-actin speed maps, and EGFP-paxillin/EGFP-vinculin (WT-vinculin/PA vinculin). Images were taken every 5 s (elapsed time shown in min:s) on an inverted microscope system (TE2000E2; Nikon) using a 100×/1.49 NA Apo TIRF objective lens. Bars: 5 µm; (flow scale bar) 2 µm*min$^{-1;}$ (speed scale) nm*min^{-1}.

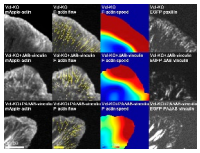

Video 6. **F-actin dynamics in *Vcl*-KO MEF expressing EGFP-ΔAB or EGFP-PA-ΔAB vinculin.** SDC-FSM time-lapse image sequences of F-actin and FA dynamics in *Vcl*-KO MEF coexpressing mApple-actin and either EFGP-paxillin (nonrescued; top), EGFP-ΔAB (middle), or EGFP-PA-ΔAB (bottom) vinculin cDNA. (left to right) mApple-actin FSM images, F-actin flow maps, F-actin speed maps, and EGFP-paxillin/-vinculin (ΔAB-/PA-ΔAB-vinculin). Images were taken every 5 s (elapsed time shown in min:s) on an inverted microscope system (TE2000E2; Nikon) using a 100×/1.49 NA Apo TIRF objective lens. Bars: 5 µm; (flow scale) 2 µm*min^{-1}; (speed scale) nm*min^{-1}.

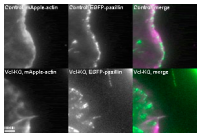

Video 7. **Nascent FA dynamics in control and *Vcl*-KO MEF.** TIRF time-lapse image sequences of nascent FA in protruding lamellipodia of control and *Vcl*-KO MEF expressing EGFP-paxillin (green) and mApple-actin (purple). Images were taken every 2 s (elapsed time shown in min:s) on an inverted microscope system (TE2000E2; Nikon) using a 100×/1.49 NA Apo TIRF objective lens. Bar, 2 µm.

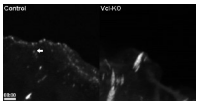

Video 8. **FA maturation in control and *Vcl*-KO MEF.** SDC fluorescence time-lapse image sequences of maturing FA in control and *Vcl*-KO MEF expressing EGFP-paxillin. Arrows indicate FA shown in Fig. 5 H. Images were taken every 20 s (elapsed time shown in min:s) on an inverted microscope system (TE2000E2; Nikon) using a 100×/1.49 NA Apo TIRF objective lens. Bar, 2 µm.

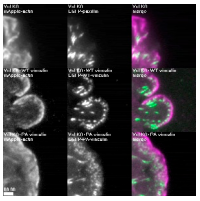

Video 9. **Nascent FA dynamics in *Vcl*-KO MEF expressing EGFP-WT or -PA vinculin.** TIRF time-lapse image sequences of nascent FA in protruding lamellipodia of *Vcl*-KO MEF coexpressing mApple-actin (purple) and either EFGP-paxillin (nonrescued; top), EGFP-WT (middle), or EGFP-PA (bottom) vinculin (green) cDNA. Images were taken every 3 s (elapsed time shown in min:s) on an inverted microscope system (Eclipse Ti; Nikon) using a 100×/1.49 NA Apo TIRF objective lens. Bar, 2 µm.

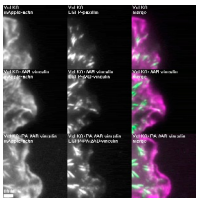

Video 10. **Nascent FA dynamics in *Vcl*-KO MEF expressing EGFP-ΔAB or EGFP-PA-ΔAB vinculin.** TIRF time-lapse image sequences of nascent FA in protruding lamellipodia of *Vcl*-KO MEF coexpressing mApple-actin (purple) and either EFGP-paxillin (nonrescued; top), EGFP-ΔAB (middle), or EGFP-PA-ΔAB (bottom) vinculin (green) cDNA. Images were taken every 3 s (elapsed time shown in min:s) on an inverted microscope system (Eclipse Ti; Nikon) using a 100×/1.49 NA Apo TIRF objective lens. Bar, 2 µm.

References

Choi, C.K., M. Vicente-Manzanares, J. Zareno, L.A. Whitmore, A. Mogilner, and A.R. Horwitz. 2008. Actin and alpha-actinin orchestrate the assembly and maturation of nascent adhesions in a myosin II motor-independent manner. *Nat. Cell Biol.* 10:1039–1050. http://dx.doi.org/10.1038/ncb1763

Ponti, A., M. Machacek, S.L. Gupton, C.M. Waterman-Storer, and G. Danuser. 2004. Two distinct actin networks drive the protrusion of migrating cells. *Science*. 305:1782–1786. http://dx.doi.org/10.1126/science.1100533

Zemljic-Harpf, A.E., J.C. Miller, S.A. Henderson, A.T. Wright, A.M. Manso, L. Elsherif, N.D. Dalton, A.K. Thor, G.A. Perkins, A.D. McCulloch, and R.S. Ross. 2007. Cardiac-myocyte-specific excision of the vinculin gene disrupts cellular junctions, causing sudden death or dilated cardiomyopathy. *Mol. Cell. Biol.* 27:7522–7537. http://dx.doi.org/10.1128/MCB.00728-07

Provided online is the computational code adhesionTracker_v1.0. This zip archive contains the complete source code for the FA detection and tracking algorithm used for the automated computation of F-actin flow velocities within segmented FA as shown in Fig. 1 E and Fig. S2, including instructions on installation and operation. The algorithm requires previous QFSM-based F-actin flow analysis. QFSM1.0.0 can be downloaded at http://lccb.hms.harvard.edu/software.html.